

# Radiological mapping in the granodiorite area of Bergama (Pergamon)-Kozak, Turkey

Özlem Karadeniz · Cüneyt Akal

Received: 27 February 2014 / Published online: 8 June 2014  
© Akadémiai Kiadó, Budapest, Hungary 2014

**Abstract** As higher radiation levels are associated with granodiorite area and the maps are more practical to interpret the results of radiological survey, the distributions of the specific activities of  $^{226}\text{Ra}$ ,  $^{232}\text{Th}$ ,  $^{40}\text{K}$  in soil-granite samples and indoor  $^{222}\text{Rn}$  activities throughout the granodiorite area of Bergama (Pergamon) were mapped in detail. Samples from the granites and soils underlying Kozak-Bergama (Pergamon) granodiorite area were collected and analyzed by HPGe gamma spectrometry system, while indoor radon levels in 20 dwellings of rural areas at this area were measured by the alpha track etch integrated method. This paper represents the baseline maps of natural radioactivity levels ( $^{226}\text{Ra}$ ,  $^{232}\text{Th}$ ,  $^{40}\text{K}$  and  $^{222}\text{Rn}$ ) and corresponding absorbed dose rates from outdoors terrestrial gamma radiation.

**Keywords** Natural radionuclides · Radon · Granodiorit · Soil · Radiological mapping · Radiological hazard

## Introduction

The external radiation exposure at the Earth's surface arises mainly from cosmic rays and from terrestrial radiation originated mainly from primordial radionuclides. Gamma-radiation from these naturally occurring radionuclides such

as  $^{40}\text{K}$ ,  $^{238}\text{U}$  and  $^{232}\text{Th}$  and their decay products, and from radionuclide deposited on the ground is the principal external source of irradiation of the human body. Terrestrial background gamma-radiation and the associated external exposure depend primarily on the local geological and geographical conditions, especially the types of rock from which the soils originate and appear at different levels of radionuclides in the soils of each region in the world [1].

High background radiation areas (HBRAs) are the special parts of the world that elevated natural background radiations are present. The high radiation levels in HBRAs arise from igneous rocks such as light-coloured volcanic rocks, granites, dark shales have higher than average uranium contents (1–3 ppm) [2, 3]. In comparison to the basaltic or ultramafic composition (<1 ppm of U), the igneous rocks of granitic composition are strongly enriched in U and Th (on an average 5 ppm of U and 15 ppm of Th) [4 and further references cited therein]. Although these radionuclides are natural, it can increase human exposure to gamma-ray radiation, when granite is used as an indoor accent material, such as a kitchen countertop. Furthermore radon gas ( $^{222}\text{Rn}$ ) and its short-lived products released from the materials can increase inhalation exposures. It has been well established that exposures to relatively high concentration of radon may lead to lung cancer in many cases [5–7]. Presently, the natural radioactive radon gas has been identified to be the second leading cause of lung cancer after tobacco smoking [8, 9] and it is well known that more than 50 % of the total radiation dose to the world population from natural sources comes from the inhalation of  $^{222}\text{Rn}$  or rather from its short-lived decay products [3].

Due to increasing concern about environmental radiological protection and the paucity of measurement data on granodiorite area of Bergama, an extensive investigation was started to determine the background radiation levels in

Ö. Karadeniz (✉)  
Department of Physics, Faculty of Sciences, Dokuz Eylül  
University, 35160 Tinaztepe, İzmir, Turkey  
e-mail: ozlem.karadeniz@deu.edu.tr

C. Akal  
Department of Geological Engineering, Engineering Faculty,  
Dokuz Eylül University, 35160 Tinaztepe, İzmir, Turkey  
e-mail: cuneyt.akal@deu.edu.tr

this region. As the spatial maps can provide significant information on pollution sources of radionuclides and the relative contribution of different sources in the environment, the distributions of the specific activities of  $^{226}\text{Ra}$ ,  $^{232}\text{Th}$ ,  $^{40}\text{K}$  in soil-granite samples and indoor  $^{222}\text{Rn}$  activities throughout the region were mapped in detail. This paper represents the baseline maps of natural radioactivity levels ( $^{226}\text{Ra}$ ,  $^{232}\text{Th}$ ,  $^{40}\text{K}$  and  $^{222}\text{Rn}$ ) and corresponding absorbed dose rates from outdoors terrestrial gamma radiation.

## Materials and methods

### Geology of Kozak granitoid pluton

Kozak Pluton—Bergama/Izmir which is located NW Anatolia, has an elliptical shape and covers an area of about 450 km<sup>2</sup> (Fig. 1). The Kozak pluton which represents a shallow level granitoid, intruded into low grade metamorphic rocks of Karakaya complex of Sakarya Tectonic Zone, consisting of Triassic aged metapelites and metabasites [12 and references there in]. Kozak pluton is surrounded by coeval dacitic–rhyolitic–andesitic–latitic volcanics and their volcanoclastic successions intercalated with lacustrine sedimentary rocks overlies the Kozak pluton. The Kozak pluton contains mafic microgranular enclaves. The enclaves are darker and fine grained. The mineralogy of enclaves is identically same with host granitoid; but the proportions of minerals are different [11]. The general mineralogical composition of the Kozak pluton is quartz, plagioclase, orthoclase, hornblende, clinopyroxene, titanite, allanite, apatite, zircon and opaque minerals. Different sized pegmatitic veins can randomly be recognized inner plutonic body and commonly observed at the contact of aplites or within the aplitic veins (Fig. 2). The general mineralogical compositions of the pegmatitic veins are consisting of K–feldspar, biotite, quartz, epidote, topaz, and pyrite. Their minerals are euhedral and vary in size between 2 and 3 cm. Geochemically the Kozak pluton is continental arc metaluminous granitoid and present granite–granodiorite to monzogranite (adamellite) compositions [11, 12]. Granitic part of the pluton which is mainly observed around Çamavlu, Yukarıcuma, Terzihalliler, Bağyüz and Okçular locations, is made up of medium- to coarse-grained (rich up to 10 mm) holocrystalline texture and has higher percentage of pinkish orthoclase (K–feldspar) crystals than granodioritic part of the pluton. The grayish-whitish granodioritic southern side of the pluton is mainly consisting of medium sized (between 3 and 4 mm) and equigranular holocrystalline texture with higher percentage of plagioclase crystals. The K–Ar ages of Kozak

Pluton using biotite and hornblende crystals range from 17.3 to 23.0 Ma [13, 14].

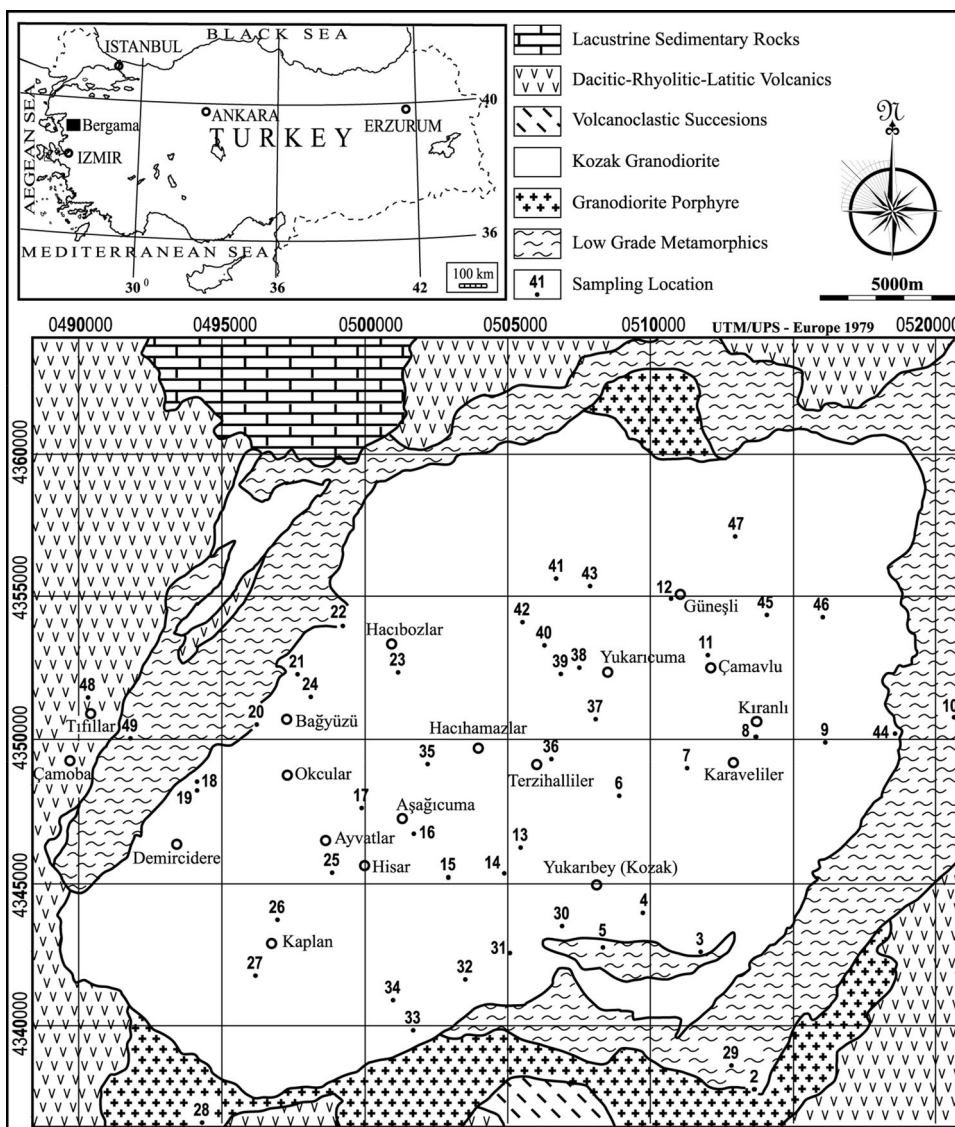
### Sample treatments and gamma-spectrometric measurements

While 37 granitoid samples were collected from the Kozak granitoid pluton, the surface soil samples up to ~10 cm depth were systematically taken (3 × 3 km grid pattern) from 49 sites distributed all over the surveyed area (Fig. 1). The location of each sample site was determined by global positioning system, GPS Garmin Model 12XL. The granite samples were first dried at room temperature, then oven dried at 105 °C until they reached a constant weight. They were crushed to a grain size of few micrometres and were then filled in a 1,000 ml Marinelli beaker. Soil samples were collected by using a spade at selected sites in forest stands. Samples of the soil were dried to a constant weight at 75 °C for 24 h in an electric oven and passed through a 2 mm sieve to eliminate impurity such as stones and roots. Each dried sample was placed in a 1,000 ml Marinelli beaker prior to analysis. The containers were sealed and stored for at least 30 days to allow for secular equilibrium between  $^{226}\text{Ra}$  and its decay products before gamma spectroscopy measurements were made.

The activity concentration of  $^{232}\text{Th}$ ,  $^{226}\text{Ra}$  and  $^{40}\text{K}$  in the soil samples were measured with a high resolution HPGe gamma-ray spectrometry system. The system was equipped with a coaxial p-type HPGe detector (AMETEC-ORTEC GEM40P4). The HPGe detector has a relative efficiency of 40 % with respect to a 3" × 3" cylindrical NaI(Tl) detector, an energy resolution of 1.85 keV at 1,332.5 keV of  $^{60}\text{Co}$  and of 0.87 keV at 122 keV of  $^{57}\text{Co}$ , a peak-to-Compton ratio of 64:1 and operating voltage 3,500 V. This detector was operated at liquid nitrogen temperature to reduce the leakage current and to increase the mobility of the charge carriers. In order to shield from photons of cosmic and terrestrial origin, the detector was covered with a 10 cm thick cylindrical lead shield with low background radiation, which is jacketed by a 9.5-mm low carbon steel outer housing. The inner lining composed of 1.5-mm-thick tin layer and 1.6-mm-thick soft copper layer to prevent interference by lead X-rays. A spectroscopic amplifier (ORTEC, Model 672), with an 16 K analog to digital converter (ASPEC-927) processed the signal. The MAESTRO-32 multichannel analyzer emulation software was utilised for peak searching, peak evaluation, energy calculation, nuclide identification, data acquisition, storage, display and on-line analysis of the spectra.

The energy calibration was obtained using standard sources from SPECTECH:  $^{60}\text{Co}$  and  $^{152}\text{Eu}$  for an energy range between 120 and 1,400 keV and analysed in the same conditions. The IAEA reference materials RGU-1

**Fig. 1** Location and map of the Kozak Pluton (modified from Akyürek [10]; Akal and Helvacı [11])



(U-ore), RGT<sub>h</sub>-1 (Th-ore) and the potassium standard was prepared from pure potassium chloride, with densities similar to the samples, were employed for the absolute efficiency calibration of the gamma spectrometry system. The reference standard sources were prepared in Marinelli beakers so as to have the same counting geometry as the samples. For the reliability of counting efficiency, additional quality control checks were confirmed using IAEA-375 reference material of known activities (424 Bq kg<sup>-1</sup> of <sup>40</sup>K, 20 Bq kg<sup>-1</sup> of <sup>226</sup>Ra and 20.5 Bq kg<sup>-1</sup> of <sup>232</sup>Th). The activities of this sample were in accordance with its certified values within error margins not exceeding 5 %.

The sample containers were placed on detector endcap for counting. The accumulating time of the sample spectra was ranged between 10,000 and 20,000 s to obtain a gamma spectrum with good statistics. To determine the background distribution due to naturally occurring

radionuclides in the environment around the detector, an empty Marinelli beaker with a volume of 1,000 ml with the same geometry was taken. This background measured during one weekend (200,000 s) was subtracted from the samples measured in order to correct the net peak area of gamma rays of the measured isotopes.

The activity concentration of <sup>226</sup>Ra was derived from the weighted average of the activities of the three gamma-ray line of 609.3, 1,120.3, 1,764.5 keV from <sup>214</sup>Bi and of one gamma-ray line of 351.9 keV from <sup>214</sup>Pb, while the gamma-ray lines of the 911.2 keV from <sup>228</sup>Ac, the 727.3 keV from <sup>212</sup>Bi, 583.2 keV and 2,614.5 keV from <sup>208</sup>Tl were used to determine the activity concentration of <sup>232</sup>Th. Several peaks from <sup>226</sup>Ra and <sup>232</sup>Th daughters were also monitored. The activity concentration of <sup>40</sup>K was obtained using its 1,461 keV gamma-ray line. The statistical errors were considered only for the counting statistical

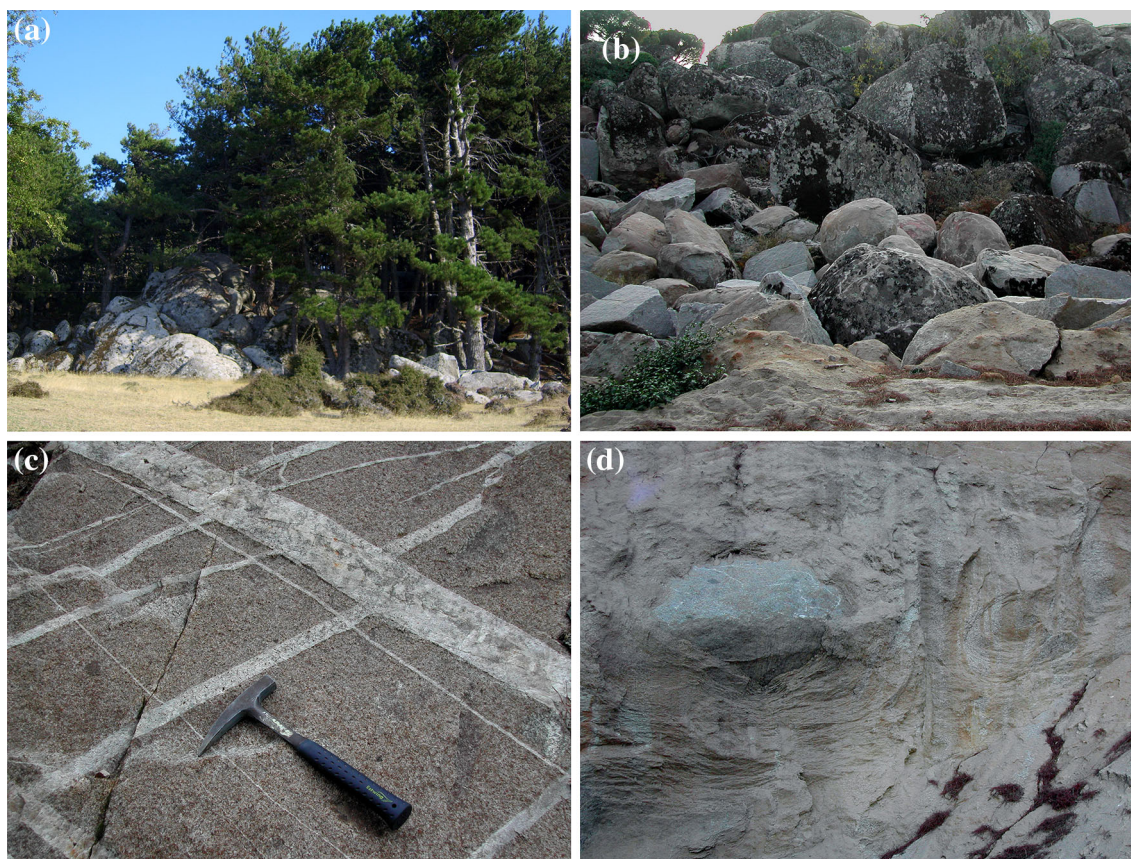


**Fig. 2** **a, b** Geomorphological arguments indicate that granitoid boulders of all sizes observed at the Kozak Pluton are still in situ. **c** Aplitic and small scaled pegmatitic veins in granite. **d** Physical and

chemical weathering process-related rounded granite boulders (core-stone) with curved shells in a matrix of weak, clayey and sandy material near Yukarıbey (Kozak) town

uncertainty, which were found in the order of 1–3 % for high activities and more than 10 % for the small activities at the 95 % level of confidence. The minimum detectable activity (MDA) based on Currie (1968) [15] for the counting time of 20,000 s was 0.17 Bq kg<sup>-1</sup> for <sup>214</sup>Pb (351 keV); 0.22, 0.59 Bq kg<sup>-1</sup> for <sup>208</sup>Tl (583, 2,614 keV); 0.21, 0.47, 0.59 Bq kg<sup>-1</sup> for <sup>214</sup>Bi (609, 1,120, 1,764 keV); 0.17 Bq kg<sup>-1</sup> for <sup>228</sup>Ac (911 keV) and 1.15 Bq kg<sup>-1</sup> for <sup>40</sup>K (1,460 keV).

#### Measurement of indoor radon

In the present study, long-term average indoor radon concentrations at 20 dwellings representative of building characteristics of the rural area were measured by using Kodak Pathé LR 115-II passive track detectors. A detailed description of the indoor radon measurement and analysis techniques used in these investigations, has been presented elsewhere [16]. As shown in Fig. 1, 18 villages located all over the Kozak/Bergama granite area, while two villages, in the regular region, have been surveyed for indoor radon measurements. Although the dwellings are formal offices,

their building characteristics are as similar as possible; all of them were built as one- or two- storeyed family houses without a basement, and constructed with brick and cement as observed with regard to most of the houses in the study area to obtain meaningful data for indoor radon.

Sampling was performed for 1 year by the same personnel during the period from 5 December 2009 to 3 December 2010 with seven sets. The radon-measuring devices were installed inside the dwellings at a height of ~1.5 m from the ground with their sensitive surfaces facing the air for an exposure period of ~30–60 days. At the end of the exposure period, the radon dosimeter with LR-115 detectors were replaced with new ones and the retrieved detectors were processed under the usual laboratory conditions. The chemical etching of the LR-115 detectors was done in 10 % NaOH solution at 60 °C for 95 min in a constant temperature etching unit with an accuracy of ±1 °C. Following the etching, detectors were then washed with distilled water and dried. Counting of the alpha tracks was done using a binocular research microscope at a magnification of 10 x 10. Background track density for the unexposed detector was separately evaluated and subtracted from the observed values.

**Table 1** Summary statistics for the activity concentration of <sup>40</sup>K, <sup>226</sup>Ra and <sup>232</sup>Th, total absorbed dose rate (D), annual effective dose equivalent (AEDE), radium equivalent activity (Ra<sub>eq</sub>), the external hazard index (H<sub>ex</sub>) and gamma index (I<sub>γ</sub>) for granite and soil samples of Bergama–Kozak

	Activity concentration (Bq kg <sup>-1</sup> )			D (nGy h <sup>-1</sup> )	AEDE (μSv y <sup>-1</sup> )	Ra <sub>eq</sub> (Bq kg <sup>-1</sup> )	H <sub>ex</sub>	I <sub>γ</sub>
	<sup>40</sup> K	<sup>226</sup> Ra	<sup>232</sup> Th	Total	Total			
<b>Granite</b>								
Median	1,037	63	85	123	151	264	0.75	0.99
Mean ± SE	1,059 ± 19	63 ± 3	85 ± 2	125	153	267	0.75	0.99
SD	114	16	15	16	19	35	0.10	0.13
GM	1,053	61	84	124	152	265	0.75	0.98
CV (%)	10.76	25.82	17.17	13	13	13	13	13
GCV(%)	10.81	26.74	17.49	13	13	13	13	13
Range	871–1,477	36–116	61–149	96–172	118–211	203–371	0.58–1.05	0.76–1.39
Skewness	1.450	1.441	2.344	1.060	1.060	1.082	1.098	1.137
Kurtosis	3.876	3.516	9.016	2.057	2.057	2.119	2.230	2.453
Frequency distribution	Log-norm	Log-norm	Log-norm					
UNSCEAR (1993) <sup>a</sup> [1]	1,200–1,800 500	100–500 50	40–350 50	120–517	150–630	250–1,139	0.7–3.1	
<b>Soil</b>								
Median	1,009	54	96	122	150	263	0.74	0.97
Mean ± SE	1,005 ± 23	58 ± 2	99 ± 5	128	157	277	0.78	1.02
SD	160	15	32	28	34	63	0.17	0.22
GM	992	56	94	126	154	270	0.76	1.00
CV (%)	15.95	25.18	32.51	21.77	22	23	22	22
GCV(%)	16.16	26.13	34.15	22.24	22	23	23	22
Range	522–1,368	37–104	31–249	61–244	74–300	128–545	0.36–1.51	0.48–1.96
Skewness	−0.047	1.176	2.247	1.519	1.519	1.653	1.582	1.540
Kurtosis	0.934	1.193	9.566	5.557	5.557	6.189	5.910	5.80
Frequency distribution	Normal	Log-norm	Log-norm					
UNSCEAR (2000) <sup>a</sup> [3]	140–850 400	17–60 35	11–64 30	10–200 60	70	≤370	< 1.0	< 1.0

Median, mean (arithmetic mean), standard error of arithmetic mean (SE), standard deviation (SD), geometric mean (GM), coefficient of variation (CV), geometric coefficient of variation (GCV), range, expressed in Bq kg<sup>-1</sup> and skewness, kurtosis of the frequency distributions of natural radionuclide activities and the radiation hazard parameters

<sup>a</sup> Typical range and mean of worldwide

**Results and discussion**

The activity concentration of natural radionuclides in granodiorites and soil

For a more general and representative overview, summary statistics for the activity concentration of <sup>40</sup>K, <sup>226</sup>Ra, <sup>232</sup>Th in granite and soil samples collected from Pergamon–Kozak granodiorite area are given in Table 1. Activity concentrations of <sup>40</sup>K in granites varied between 871 ± 8 and 1,477 ± 11 Bq kg<sup>-1</sup> with a geometric mean of 1,053 Bq kg<sup>-1</sup>, while the ranges of <sup>226</sup>Ra and <sup>232</sup>Th concentrations were 36 ± 3–116 ± 3 with a geometric mean of 61 Bq kg<sup>-1</sup> and 61 ± 4–149 ± 6 Bq kg<sup>-1</sup> with a geometric mean of 84 Bq kg<sup>-1</sup>, respectively (Table 1). The

results presented in this paper are in general agreement with the first measurements of activity concentrations of naturally occurring radionuclides in 11 granitoid samples from characteristic geological rock types of Pergamon–Kozak granodiorite area reported by Karadeniz et al. (2011) [17]. These values are hardly distinct from the typical range of similar published studies [17 and further references cited therein; 18], and the worldwide concentrations reported by UNSCEAR [1].

Values of <sup>40</sup>K activity concentration in soils varied from 522 ± 7 to 1,368 ± 12 Bq kg<sup>-1</sup> with a mean of 1,005 Bq kg<sup>-1</sup>, while the ranges of <sup>226</sup>Ra and <sup>232</sup>Th concentrations were 37 ± 3–104 ± 4 with a geometric mean of 56 Bq kg<sup>-1</sup> and 31 ± 4–249 ± 8 Bq kg<sup>-1</sup> with a geometric mean of 94 Bq kg<sup>-1</sup>, respectively. It is important to

note that the estimations on all mean concentrations of  $^{226}\text{Ra}$ ,  $^{232}\text{Th}$  and  $^{40}\text{K}$  in soil in areas of normal radioactivity given in the recent UNSCEAR 2000 report [3] are 35, 30 and 400  $\text{Bq kg}^{-1}$ , respectively, and typical ranges are 17–60  $\text{Bq kg}^{-1}$  for  $^{226}\text{Ra}$ , 11–64  $\text{Bq kg}^{-1}$  for  $^{232}\text{Th}$  and 140–850  $\text{Bq kg}^{-1}$  for  $^{40}\text{K}$ . In the light of the above knowledge, only for  $^{226}\text{Ra}$  the values obtained fall within the typical range of worldwide average values.

The frequency distributions of the  $^{40}\text{K}$ ,  $^{226}\text{Ra}$  and  $^{232}\text{Th}$  activities granite and soil samples were studied. The measured histograms were compared with the normal and log-normal distribution functions using Kolmogorov–Smirnov test values for the goodness-of-fit [19]. Accordingly, the values of the coefficients of skewness and kurtosis, and the type of the frequency distributions were also summarised in Table 1. Application of the Kolmogorov–Smirnov test and the approximate null value of the skewness coefficient obtained for  $^{40}\text{K}$  activities of soils show that this distribution is practically symmetrical, while the positive values obtained in the statistics of other natural radionuclide activities in granite and soil samples indicate that the distribution is asymmetric. Because the results fit to a log-normal distribution fairly well, it is convenient to use the geometric mean values as a mean rather than arithmetic mean [20].

An analysis of the correlation between the specific activities of  $^{40}\text{K}$ ,  $^{226}\text{Ra}$  and  $^{232}\text{Th}$  in the granitoid and soil samples is shown in Fig. 3. In soils, the best-fitting relation between  $^{232}\text{Th}$  and  $^{40}\text{K}$  versus  $^{226}\text{Ra}$  was of linear and positive type, with a correlation coefficient 0.543 and 0.235, respectively. There was a good correlation ( $R^2 = 0.717$ ) between the activity concentrations of  $^{232}\text{Th}$  and  $^{40}\text{K}$  in the granitoid samples. Other investigated relations also represent the positive trend but are rather weak, as agreed with previous studies [21, 22].

The specific levels of terrestrial environmental radiation are related to the geological composition of each lithologically separated area, and to the content in thorium (Th), uranium (U) and potassium (K) of the rock from which the soils originate in each area [23]. The analysis of the NORM relative abundance (Th/U, K/U and K/Th ratios) may also give information on the relative enrichment/depletion processes as a result of the complex metamorphic history, alteration and/or weathering, which affected the investigated rocks. In addition, these patterns can delineate areas of potential mineralization, which are not restricted to U and Th minerals [24–26].

As mentioned reasons above, it is preferable that the results are expressed in terms of equivalent uranium, equivalent thorium concentrations and percent (%) K. By gamma spectrometric analyses of  $^{40}\text{K}$ ,  $^{214}\text{Bi}$  and  $^{208}\text{Tl}$ , assuming radioactive equilibrium, the surface abundance of

K, U, and Th can be determined, expressed as percent (%) K, ppm equivalent uranium (eU) and ppm equivalent thorium (eTh) respectively [27]. To convert K (%) in  $^{40}\text{K}$  activity concentration, ppm equivalent uranium (eU) in  $^{238}\text{U}$  activity concentration and ppm equivalent thorium (eTh) in  $^{232}\text{Th}$  activity concentration, the conversion factors are, respectively, 309.3 ( $\text{Bq kg}^{-1}$ )/(%) for K, 12.3 ( $\text{Bq kg}^{-1}$ )/(mg  $\text{g}^{-1}$ ) for U and 4.1 ( $\text{Bq kg}^{-1}$ )/(mg  $\text{g}^{-1}$ ) for Th, as well as their decay products under secular equilibrium conditions of these natural series [18]. Accordingly, elemental concentrations are converted in units of 1  $\mu\text{g g}^{-1}$  (equivalent to ppm) for thorium and uranium, and as a percentage (%) for potassium.

In the area under investigation, the mean eTh (ppm), eU (ppm) and K (%) concentrations in the granitic rocks were 21, 5 ppm and 3 (%), respectively. It is well known that igneous rocks of granitic composition are strongly enriched in Th and U (on an average 15 ppm of Th and 5 ppm of U), compared to rocks of basaltic or ultramafic composition (<1 ppm of U). The eTh/eU concentration ratios of the granitoid samples varied from 2.10 to 9.92 with a mean value of 4.29, while the mean eTh (ppm)/K (%) concentration ratio was 6.07. These mean concentration ratios indicate acid igneous rocks according to Clark [28]. It may be useful to remember that the theoretically expected eTh/eU ratio for normal continental crust is about 3.0 and the eTh/eU ratios close to 3.5 (Clark's value) in the granitoid samples denotes a slight enrichment of uranium [23]. On the other hand, the eTh (ppm)/K (%) ratio is presented to be 4.5 in acid igneous rocks by Clark (1966) [28].

The eTh/eU ratios in the soils varied from 2.08 to 7.37 with a mean value of 5.12 in the surveyed soil samples. Accordingly, Th/U ratio for the soil samples overlying the acidic igneous rocks indicated that a relationship exists between the parent materials and the soils. The current study showed that the eTh (ppm)/K (%) ratio of the soils in the Pergamon–Kozak granodiorite area appeared in the range of 3.81–16.89 with a mean value of 7.46. These results point out that there is an enrichment of the thorium in the studied area and the thorium is the dominant source of the gamma radiation as mentioned in similar published study [20].

#### The radiation hazard parameters

The dose rates at 1 m above the ground level resulting from the gamma emitting radionuclides in the  $^{40}\text{K}$ ,  $^{226}\text{Ra}$  and  $^{232}\text{Th}$  for uniform distribution in soil profile were calculated from concentrations of these radionuclides using the following equation [3];

$$D(\text{nGy h}^{-1}) = 0.0417 C_{\text{K}} + 0.462 C_{\text{Ra}} + 0.604 C_{\text{Th}}, \quad (1)$$

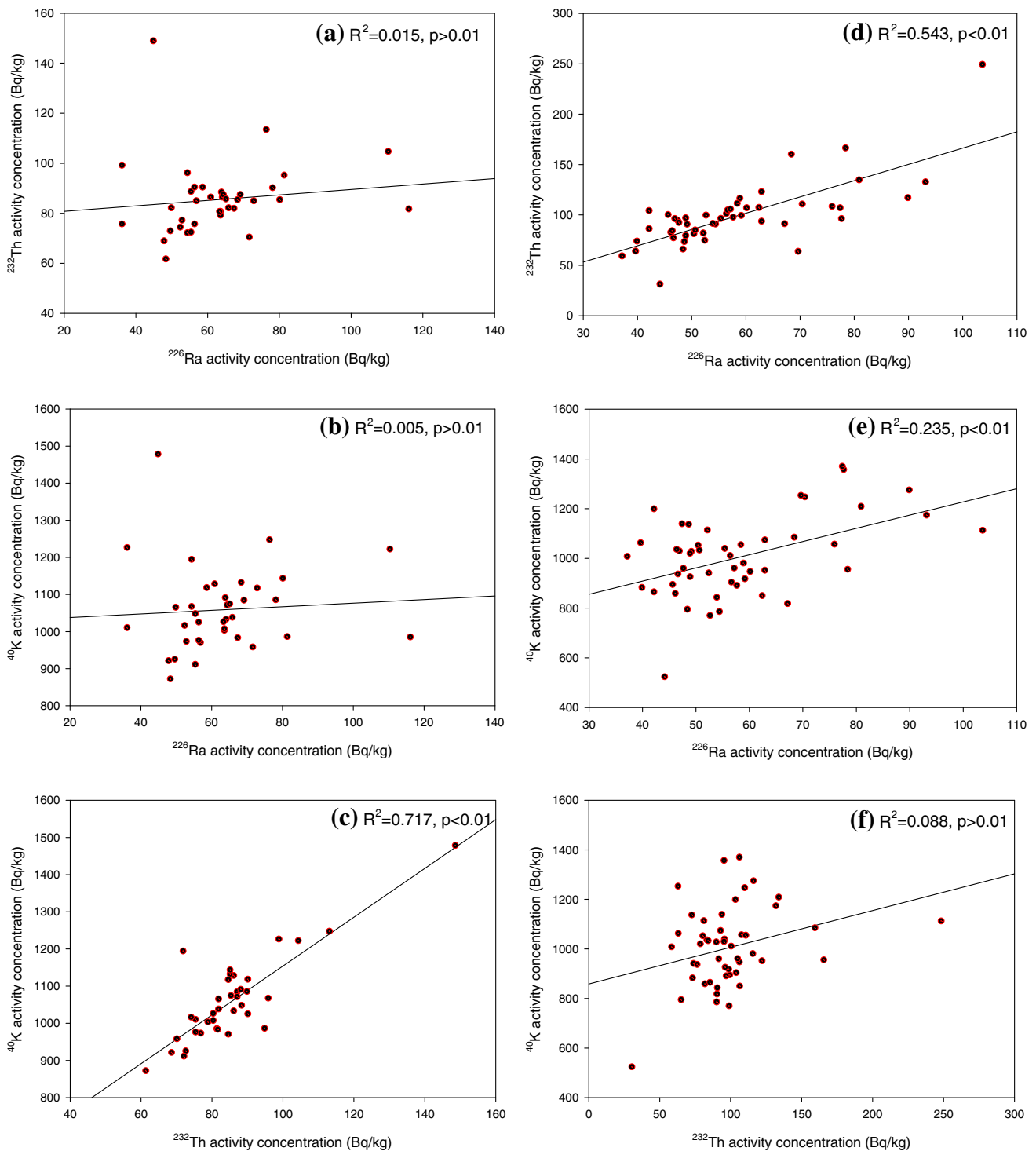


**Fig. 3** Scatter plot of granitoid  $^{226}\text{Ra}$  versus granitoid  $^{232}\text{Th}$  (a); granitoid  $^{226}\text{Ra}$  versus granitoid  $^{40}\text{K}$  (b); granitoid  $^{232}\text{Th}$  versus granitoid  $^{40}\text{K}$  (c); soil  $^{226}\text{Ra}$  versus soil  $^{232}\text{Th}$  (d); soil  $^{226}\text{Ra}$  versus soil  $^{40}\text{K}$  (e); soil  $^{232}\text{Th}$  versus soil  $^{40}\text{K}$  with linear regression lines

where  $D$  is the dose rate in air outdoors,  $C_K$ ,  $C_{\text{Ra}}$  and  $C_{\text{Th}}$  the activity concentrations of  $^{40}\text{K}$ ,  $^{226}\text{Ra}$  and  $^{232}\text{Th}$  in the soil sample, respectively. During calculation, secular equilibrium was assumed to exist between radionuclides and their progeny within each series.

As seen in Table 1, the outdoor absorbed dose rate in air outdoors just from the terrestrial radionuclides in soils ranged between 61 and 244  $\text{nGy h}^{-1}$  with a mean of 128  $\text{nGy h}^{-1}$  and found to be within the typical range of worldwide average values (10–200) [3]. Concerning the

**Table 2** Summary statistics for the  $^{222}\text{Rn}$  activity concentration ( $\text{Bq m}^{-3}$ ) data on dwellings of Bergama–Kozak during the monitoring period from 5 December 2009 to 3 December 2010

	$^{222}\text{Rn}$ activity concentration ( $\text{Bq m}^{-3}$ )
Median	77
Arithmetic mean $\pm$ SE	101 $\pm$ 16
SD	72
Geometric mean	83
CV (%)	71
GCV(%)	86
Range	31–285
Skewness	1,812
Kurtosis	3,448
Frequency distribution	Log-normal

Median, arithmetic mean, standard error of arithmetic mean (SE), standard deviation (SD), geometric mean (GM), coefficient of variation (CV), geometric coefficient of variation (GCV), range, expressed in  $\text{Bq m}^{-3}$  and skewness, kurtosis of the frequency distributions of indoor  $^{222}\text{Rn}$  activity concentrations

granites, absorbed dose rate in air outdoors ranged between 96 and 172  $\text{nGy h}^{-1}$  with a mean of 125  $\text{nGy h}^{-1}$ . These values are within the range for the granite rocks specified by UNSCEAR 1993 report [1].

In the UNSCEAR 2000 Report [3], a coefficient of 0.7  $\text{Sv Gy}^{-1}$  was used to convert absorbed dose in air to effective dose equivalent for environmental exposures to gamma rays of moderate energy. Taking the outdoor occupancy factor to be 0.2, the annual effective dose equivalent from outdoors in units of  $\mu\text{Sv}$  is calculated by the following formula:

$$\begin{aligned} \text{Effective dose rate}(\mu\text{Sv a}^{-1}) &= \text{Dose rate}(\text{nGy h}^{-1}) \\ &\times 8760(\text{h a}^{-1}) \times 0.2(\text{occupancy factor}) \\ &\times 0.7 \text{ Sv Gy}^{-1}(\text{conversion coefficient}) \times 10^{-3} \end{aligned} \quad (2)$$

In this regard, the annual effective dose from external exposure to terrestrial radionuclides in the surveyed granodiorite area ranging from 74 to 300  $\mu\text{Sv y}^{-1}$  with a mean value of 157  $\mu\text{Sv y}^{-1}$  for soils, while ranging from 118 to 211  $\mu\text{Sv y}^{-1}$  with a mean value of 153  $\mu\text{Sv y}^{-1}$  for granites.

The gamma-ray radiation hazards due to the specified radionuclides were assessed by currently used indices as radium-equivalent activity ( $\text{Ra}_{\text{eq}}$ ) and external radiation hazard ( $H_{\text{ex}}$ ). The  $\text{Ra}_{\text{eq}}$  of a sample is given by [29, 30]

$$\text{Ra}_{\text{eq}} = 0.077 C_{\text{K}} + C_{\text{Ra}} + 1.43 C_{\text{Th}} \quad (3)$$

where  $C_{\text{K}}$ ,  $C_{\text{Ra}}$  and  $C_{\text{Th}}$  and are the average activity concentrations of  $^{40}\text{K}$ ,  $^{226}\text{Ra}$  and  $^{232}\text{Th}$ , in  $\text{Bq kg}^{-1}$ , respectively. Estimated  $\text{Ra}_{\text{eq}}$  values for the collected samples varied from 128 to 545  $\text{Bq kg}^{-1}$  (Table 1) and some values

are higher than the recommended maximum value of 370  $\text{Bq kg}^{-1}$  [29, 31].

To limit the annual external gamma-ray dose (UNSCEAR, 1982) [32] to 1.5  $\text{mGy}$  for the samples under investigation, the external hazard index ( $H_{\text{ex}}$ ) is given by the following equation:

$$H_{\text{ex}} = C_{\text{K}}/4810 + C_{\text{Ra}}/370 + C_{\text{Th}}/259 \leq 1, \quad (4)$$

The results of  $H_{\text{ex}}$  based on the criterion formula [Eq.(4)] range from 0.36 to 1.51 (Table 1).

The gamma index ( $I_{\gamma}$ ) proposed by the European Commission (1999) [33] is defined in order to assess gamma-ray radiation originating from building materials. For a typical material it is given by the following expression:

$$I_{\gamma} = \frac{C_{\text{Ra}}}{300} + \frac{C_{\text{Th}}}{200} + \frac{C_{\text{K}}}{3000} \quad (5)$$

where,  $C_{\text{Ra}}$ ,  $C_{\text{Th}}$  and  $C_{\text{K}}$  are the specific activities of  $^{226}\text{Ra}$ ,  $^{232}\text{Th}$  and  $^{40}\text{K}$ , respectively. The values 300, 200 and 3,000  $\text{Bq kg}^{-1}$  were calculated for a dose criteria limit of 1  $\text{mSv y}^{-1}$ . Based on the these criterion, Table 1 indicates that  $I_{\gamma}$  is ranged from 0.76 to 1.39 and  $I_{\gamma}$  values are less than unity in granite samples except for six samples. Therefore, most of the granite samples are safe and can be used as a construction material without posing any significant radiological threat to the population.

#### Indoor radon concentrations

The values of indoor radon concentrations calculated for the Kozak-Bergama (Pergamon) granodiorite area are ranged from 11  $\pm$  1 to 2,549  $\pm$  38  $\text{Bq m}^{-3}$  during the monitoring period from from 5 December 2009 to 3 December 2010. There was a large variation in the values of radon concentration between the dwellings in different villages of Kozak. It is well known that the radon concentration in the indoor air depend strongly on geological and geophysical conditions, it may vary with building ageing, height above the ground, ventilation pattern, architectural style of building (materials of construction and soil concentration), heating systems, the meteorological conditions such as temperature, barometric pressure, wind speed, rainfall and even variation of the living habits of the occupants [34–38]. The minimum value of the average radon concentration (31  $\text{Bq m}^{-3}$ ) has been recorded in the Ayvatlar village, whereas the maximum value (1,003  $\text{Bq m}^{-3}$ ) has been found in the Terzihaliler village. Only two of the dwellings was having a concentration of radon more than the action level (200  $\text{Bq m}^{-3}$ ) as recommended by the International Commission on Radiation Protection [39] and one of the dwellings was having a concentration of radon more than the activity level of



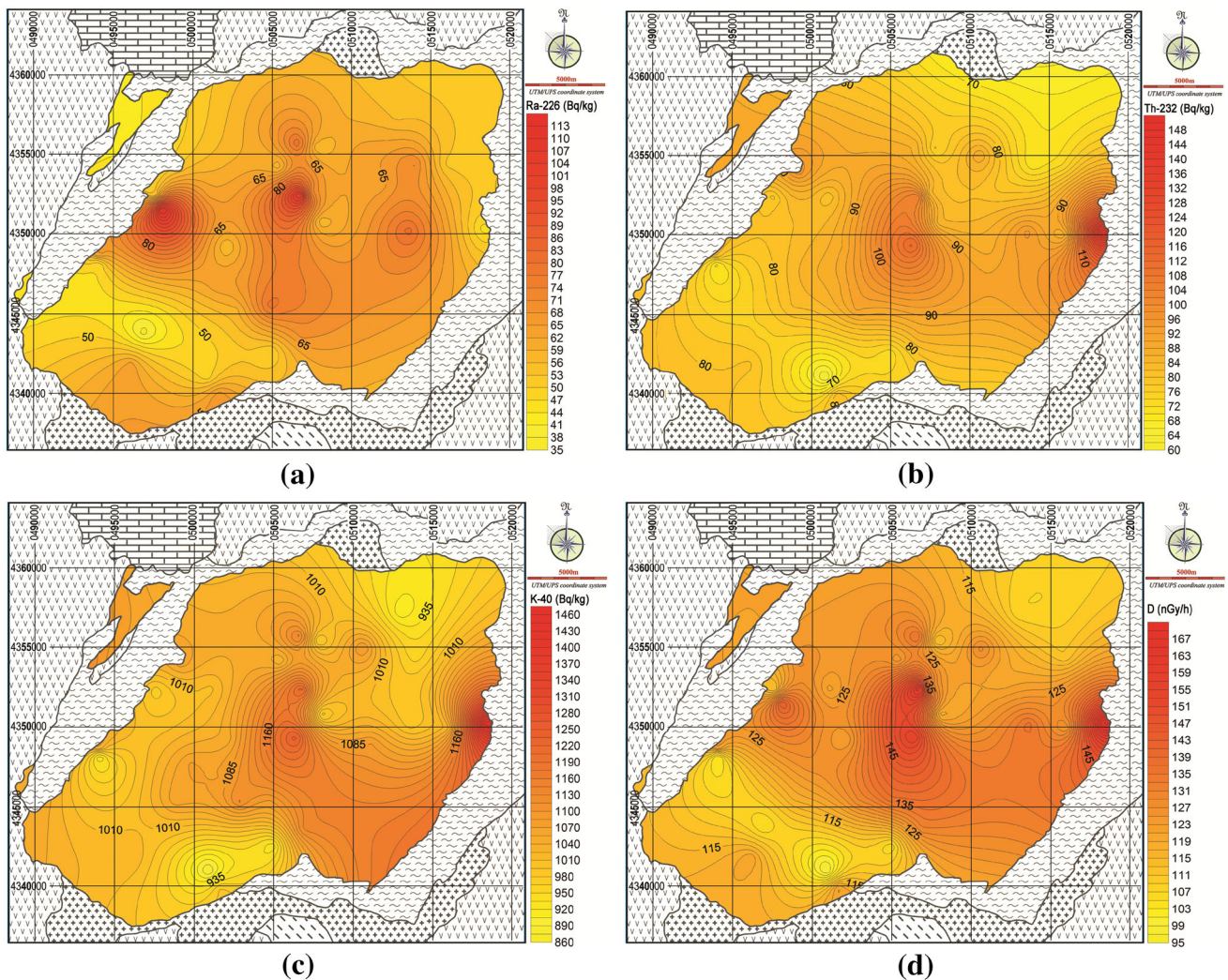


**Fig. 4** Interpolated radiological maps of **a**  $^{226}\text{Ra}$ , **b**  $^{232}\text{Th}$ , **c**  $^{40}\text{K}$  activity concentrations and **d** outdoor gamma dose rates, determined from 37 granitoid samples in the Kozak/Bergama granite area

400 Bq m<sup>-3</sup> given by the Turkish Atomic Energy Commission. Results obtained in the current survey have been compared with the data published at the national and international levels. After excluding the values of Terzihaliler village, the geometric mean was found to be 83 Bq m<sup>-3</sup>, while the arithmetic mean was 101 Bq m<sup>-3</sup> (Table 2). The average radon concentration value (83 Bq m<sup>-3</sup>) is higher than those reported for some other HBRA of the world [40, 41] and the world mean value of 40 Bq m<sup>-3</sup> [3]. These high radon levels may be due to the high radium contents in the soil of the local area and the poor ventilation of houses. On the other hand, the average indoor radon concentration value obtained from this study is lower than the values reported for some other granitic areas of the world [42] and some other provinces of Turkey [43]. Distribution of indoor radon levels follows a log-normal distribution as confirmed by the applied

Kolmogorov–Smirnov normality test ( $p > 0.05$ ). The values of the geometric mean and the median from Table 2 are appropriate for characterising this type of distribution also.

The exposures and consequent doses from radon are estimated from the measured indoor radon concentrations. Accordingly, the average annual effective dose was calculated using the dose conversion factor of 9 nSv (Bq h m<sup>-3</sup>)<sup>-1</sup> with an indoor occupancy factor of 0.8, assuming the equilibrium factor value of 0.4 based on the recent UNSCEAR (2000) report [3]. The distribution of the measured values predicted that the time-integrated  $^{222}\text{Rn}$  concentrations range from 11 ± 1 to 2,549 ± 38 Bq m<sup>-3</sup>. This corresponds to an annual effective dose equivalent ranging from 0.27 to 64.31 mSv.

The ICRP has given general recommendations concerning the problem of indoor radon and recommended that

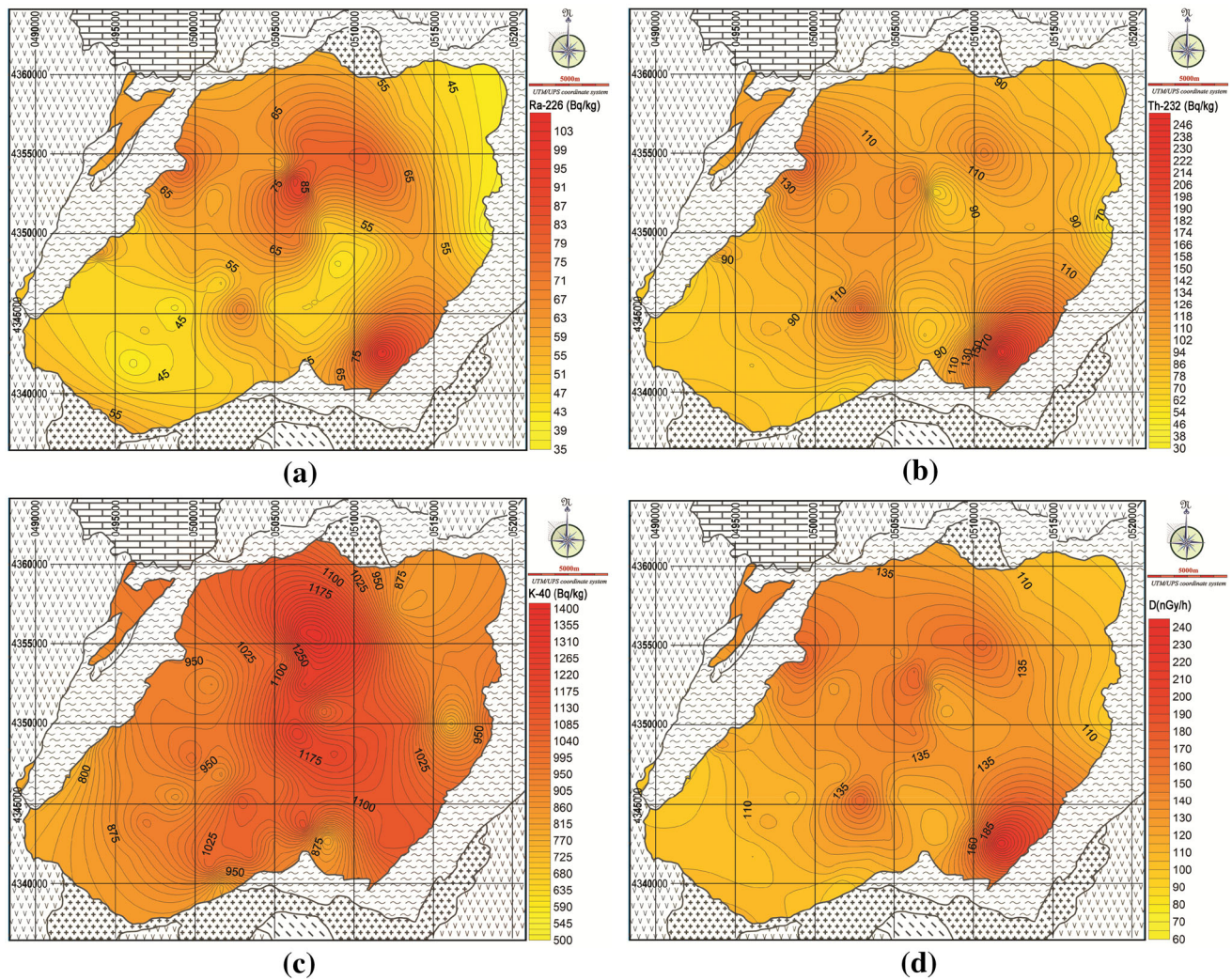


**Fig. 5** Interpolated radiological maps of **a**  $^{226}\text{Ra}$ , **b**  $^{232}\text{Th}$ , **c**  $^{40}\text{K}$  activity concentrations and **d** outdoor gamma dose rates, determined from 49 soil samples in the Kozak/Bergama granite area

remedial action against radon is always justified above a continued effective dose of 10 mSv, while an action level within the range 3–10 mSv  $\text{y}^{-1}$  has been proposed [39]. The highest average annual effective dose from the inhalation of radon was found for the Terzihaliler village: from 5.96 to 64.31 mSv. Thus, for all the villages of the study area, the annual effective dose received by the residents lies in the range of the action level. The average of dose values in the area is 2.54 mSv  $\text{y}^{-1}$ , and is higher than the world average of 1.15 mSv  $\text{y}^{-1}$  [3]. The value of Terzihaliler was not taken into account, as it is expected to be non-representative.

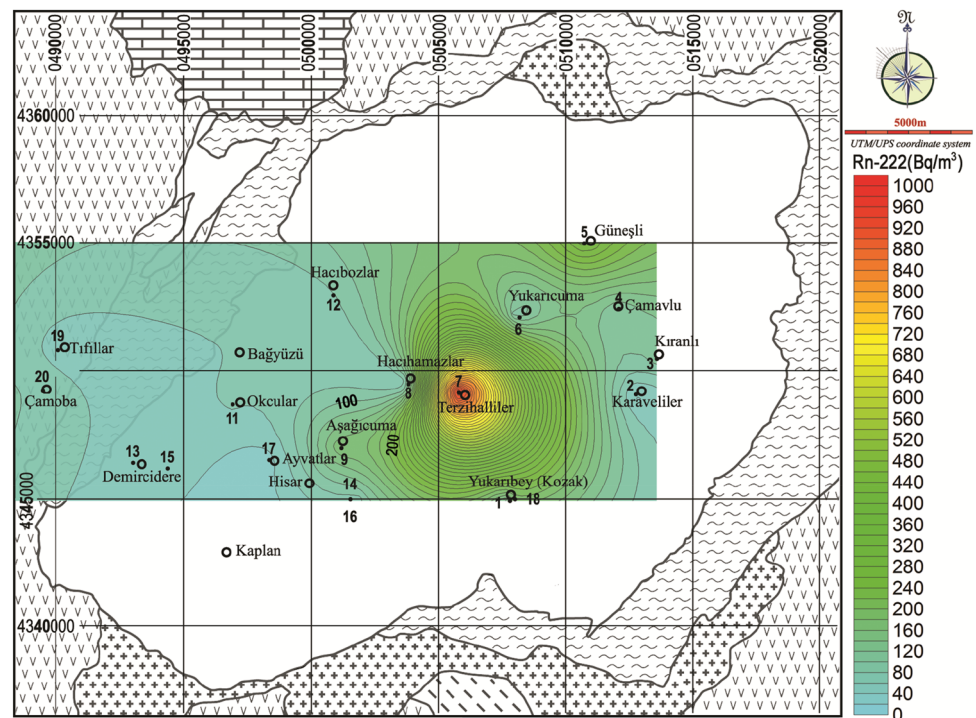
The radiological maps

The use of gamma ray spectrometry for quantitative mapping of surface radioelement distribution was established

during the late 1960s. The naturally occurring radioelements are of considerable geochemical significance, because of their almost ubiquitous distribution and sensitivity as indicators of geological processes. Spatial radioelement patterns can be used to differentiate lithologies and indicate zones of alteration. Interpreted in conjunction with other data these patterns can delineate areas of potential mineralization, which are not restricted to U and Th minerals [27]. Consequently, radiological mapping data for the region are pointed out that, the distributions of the  $^{232}\text{Th}$ ,  $^{226}\text{Ra}$  and  $^{40}\text{K}$  activities and gamma dose rate as well show a discrepancy generally owing to differences in basic geology.

The distributions of the natural radioactivity as well as the corresponding absorbed dose rates from outdoors terrestrial gamma radiation throughout the region are mapped in detail as illustrated in Figs. 4, 5, 6. The results of host

**Fig. 6** Interpolated radiological map of  $^{222}\text{Rn}$  activity concentrations determined from 20 villages located all over the Kozak/Bergama granite area



rock granitoid suggest that the granitic parts of the pluton have the highest anomalies of  $^{232}\text{Th}$ ,  $^{226}\text{Ra}$  and  $^{40}\text{K}$ . Rest of the Kozak pluton which corresponds to granodioritic parts of the pluton has low concentration values. The  $^{226}\text{Ra}$  and  $^{232}\text{Th}$  activities of soil samples almost present same values but related with tick of soil layer the values getting higher in the area which are related with concentration of heavy minerals such as sphene and zircon crystals. The maximum  $^{40}\text{K}$  activities are same but as seen Figs. 4, 5, the average value of soil samples is higher than host rock granitoid, these widespread high anomalies are related with the presence of thick soil layer which have got richer by biotite and amphibole crystals.

## Conclusion

Due to an increased use of natural stone products as decorative building materials and the paucity of measurement data on granodiorite area of Bergama, an extensive investigation was started to determine the background radiation levels in granite samples of wide use locally and soil samples at the granodiorite area of Bergama (Pergamon). Keeping in view the health hazardous effects of radon, the indoor radon measurements were also made by a time-integrated method using SSNTDs at 20 dwellings in the villages of Kozak-Bergama. This paper represents the detailed maps of natural radioactivity levels ( $^{226}\text{Ra}$ ,  $^{232}\text{Th}$ ,  $^{40}\text{K}$  and  $^{222}\text{Rn}$ ) and corresponding radiological parameters.

In the present study,  $^{40}\text{K}$ ,  $^{226}\text{Ra}$  and  $^{232}\text{Th}$  activity concentrations in granites are hardly distinct from the worldwide concentrations for  $^{40}\text{K}$ ,  $^{226}\text{Ra}$  and  $^{232}\text{Th}$ , reported by UNSCEAR 1993 as 1,200–1,800, 100–500 and 40–350  $\text{Bq kg}^{-1}$ , respectively. The radiological parameters such as radium equivalent activity ( $Ra_{eq}$ ), external hazard index ( $H_{ex}$ ) and gamma index ( $I_\gamma$ ) for granites are acceptable for safe use as construction materials according to the dose criteria limits proposed by OECD and European Commission. The observed mean concentration of  $^{226}\text{Ra}$  in the soil samples fall within the typical range of worldwide average values, while the mean  $^{232}\text{Th}$  and  $^{40}\text{K}$  activities of soil samples were higher than the universal typical ranges. The corresponding dose rates and the average effective dose equivalent were less than their respective limiting values. Consequently, surveyed area has no significant hazard from health point of view.

The average radon concentration level ( $83 \text{ Bq m}^{-3}$ ) in the studied area was higher than the world mean value of  $40 \text{ Bq m}^{-3}$ . If the recommendations made by the ICRP ( $200 \text{ Bq m}^{-3}$ ) and the Turkish Atomic Energy Commission ( $400 \text{ Bq m}^{-3}$ ) are followed, then all of the dwellings surveyed were generally within the safe limits. In all the villages of the study area, except one, the annual effective dose received by the residents lies in the range of the action level given by ICRP, while the average of the dose values ( $2.54 \text{ mSv y}^{-1}$ ) in the area is higher than the world average of  $1.15 \text{ mSv y}^{-1}$ .

As the spatial maps are more practical to interpret the results of radiological survey, the distributions of the

specific activities of  $^{226}\text{Ra}$ ,  $^{232}\text{Th}$ ,  $^{40}\text{K}$  in soil-granite samples throughout the region were mapped in detail. The results of host rock granitoid suggest that the granitic parts of the pluton have the highest anomalies of  $^{232}\text{Th}$ ,  $^{226}\text{Ra}$  and  $^{40}\text{K}$ . The  $^{226}\text{Ra}$  and  $^{232}\text{Th}$  activities of soil samples almost present same values but related with tick of soil layer the values getting higher in the area which are related with concentration of heavy minerals such as sphene and zircon crystals. Widespread high  $^{40}\text{K}$  anomalies of soil samples are related with the presence of thick soil layer which have got richer by biotite and amphibole crystals.

**Acknowledgments** Grateful thanks are offered to the provider of financial support for the research presented here: Dokuz Eylül University Scientific Research Project (Project no: 2009.KB.FEN.039). The authors are also grateful to Prof. Dr. Günseli Yaprak for professional advice on several aspects of the Gamma spectroscopy and radon measurements, to Dr. Cem Kincal for his indispensable help in drawing radiological maps and to the graduate and under graduate students; Miss. Nazan Çıyırak, Mrs. İpek Emen Zeytüncü, Mr. Yiğit Nalbant, Mr. Sadi Deniz Kayhan and Mr. Onur Büyükkök for assisting in sample collection, preparation of granites and soils.

## References

1. UNSCEAR (1993) Sources and biological effects of ionizing radiation. Report to general assembly, with scientific annexes, United Nations, New York
2. WHO (1988) Technical report. Indoor air quality: Radon—Report on a WHO working group. J Environ Radioact 73–91 (document by the WHO Regional Office for Europe)
3. UNSCEAR (2000) Sources and biological effects of ionizing radiation. Report to general assembly, with scientific annexes, United Nations, New York
4. Aydarous ASH, Zeghib S, Al-Dughmah M (2010) Measurements of natural radioactivity and the resulting radiation doses from commercial granites. Radiat Prot Dosim 142(2–4):363–368
5. Pershagen G, Liang ZH, Hrubec Z, Svensson C, Boice JD Jr (1992) Residential radon exposure and lung cancer in Swedish women. Health Phys 63:179–186
6. Field RW, Steck DJ, Smith BJ, Brus CP, Fisher EF, Neuberger JS, Lynch CF (2001) The Iowa radon lung cancer study-phase I: residential radon gas exposure and lung cancer. Sci Total Environ 272:67–72
7. Planinic J, Faj D, Vukovic B, Faj Z, Radolic V, Suveljak B (2003) Radon exposure and lung cancer. Radioanal Nucl Chem 256(2):349–352
8. IARC (International Agency for Research on Cancer) (1988) Radon and manmade mineral fibres. Monographs on the evaluation of carcinogenic risks to humans, vol. 43. IARC, Lyon. ISBN 92-832-1243-6
9. NRPB (2000) Health risks from radon. National Radiological Protection Board, UK
10. Akyürek B, Soysal Y (1983) Biga yarımadası güneyinin (Savastepe–Kırkağaç–Bergama–Ayvalık) temel jeoloji özellikleri. Bull Miner Res Explor 95/96: 1–12
11. Akal C, Helvacı C (1999) Mafic microgranular enclaves in the Kozak granodiorite, Western Anatolia. Turk J Earth Sci 8:1–17
12. Altunkaynak Ş, Yılmaz Y (1998) The mount Kozak magmatic complex, Western Anatolia. J Volcanol Geotherm Res 85:211–233
13. Delaloye M, Bingöl E (2000) Granitoids from western and northwestern Anatolia: geochemistry and modelling of geodynamic evolution. Int Geol Rev 42:241–268
14. Boztuğ D, Harlavan R, Jonckheere R, Can İ, Sarı R (2009) Geochemistry and K-Ar cooling ages of the Ilica, Çataldağ (Balıkesir) and Kozak (Izmir) granitoids, West Anatolia, Turkey. Geol J 44:79–103
15. Currie LA (1968) Limits for qualitative detection and quantitative determination. Anal Chem 40(3):586–593
16. Karadeniz Ö, Yaprak G, Akal C, Emen İ (2012) Indoor radon measurements in the granodiorite area of Bergama (Pergamon)-Kozak, Turkey. Radiat Prot Dosim 149(2):147–154
17. Karadeniz Ö, Çıyırak N, Yaprak G, Akal C (2011) Terrestrial gamma exposure in the granodiorite area of Bergama (Pergamon)-Kozak, Turkey. Radioanal Nucl Chem 288(3):919–926
18. Canbaz B, Çam NF, Yaprak G, Candan O (2010) Natural radioactivity ( $^{226}\text{Ra}$ ,  $^{232}\text{Th}$  and  $^{40}\text{K}$ ) and assessment of radiological hazards in the Kestanbol granitoid, Turkey. Radiat Prot Dosim 141(2):192–198
19. Karadeniz Ö, Yaprak G (2007) Distribution of radiocesium and natural gamma emitters in pine needles in coniferous forest sites of Izmir. Appl Radiat Isot 65(12):1363–1367
20. Öztürk BC, Çam NF, Yaprak G (2013) Reference levels of natural radioactivity and  $^{137}\text{Cs}$  in and around the surface soils of Kestanbol pluton in Ezine region of Çanakkale province, Turkey. J Environ Sci Health Pt A 48:1522–1532
21. Rahman SU, Matiullah Malik F, Rafique M, Anwar J, Ziafat M, Jabbar A (2011) Measurement of naturally occurring/fallout radioactive elements and assessment of annual effective dose in soil samples collected from four districts of the Punjab Province, Pakistan. J Radioanal Nucl Chem 287:647–655
22. Jabbar A, Arshed W, Bhatti AS, Ahmad SS, Rehman SU, Dilband M (2010) Measurement of soil radioactivity levels and radiation hazard assessment in mid Rechna interfluvial region, Pakistan. J Radioanal Nucl Chem 283:371–378
23. Tzortzis M, Tsertos H (2004) Determination of thorium, uranium and potassium elemental concentrations in surface soils in Cyprus. J Environ Radioact 77:325–338
24. Verdoya M, Chiozzi P, Pasquale V (2001) Heat-producing radionuclides in metamorphic rocks of the Briançonnais-Piedmont Zone (Maritime Alps). Eclogae Geol Helv 94:1–7
25. Chiozzi P, Pasquale V, Verdoya M (2002) Naturally occurring radioactivity at the Alps-Apennines transition. Radiat Meas 35:147–154
26. Alnour IA, Wagiran H, Ibrahim N, Laili Z, Omar M, Hamzah S, Idi BY (2012) Natural radioactivity measurements in the granite rock of quarry sites, Johor, Malaysia. Radiat Phys Chem 81:1842–1847
27. A global geochemical database for environmental and resource management, final report of IGCP Project 259, (1995). (<http://unesdoc.unesco.org/images/0010/001010/101010eo.pdf>)
28. Clark SP, Peterman ZK, Heier KS (1966) Abundances of uranium, thorium and potassium. In: Clark SP (ed) Handbook of physical constants. Geol Soc Am Mem 47:521–541
29. Beretka J, Mathew PJ (1985) Natural radioactivity of Australian building materials, industrial wastes and by-products. Health Phys 48:87–95
30. Krieger R (1981) Radioactivity of construction materials. Betonwerk Fertigteile-Tech 47:468
31. OECD (1979) Nuclear energy agency. Exposure to radiation from natural radioactivity in building materials. Report by NEA group of experts (Paris, France: OECD)
32. UNSCEAR (1982) Sources and biological effects of ionizing radiation. Report to general assembly, with scientific annexes, United Nations, New York

33. EC (European Commission) (1999) Radiation protection 112. Radiological protection principles concerning the natural radioactivity of building materials directorate-general environment, nuclear safety and civil protection
34. Mishra R, Tripathy SP, Pachua L, Laldawngliana C, Lalramengzami R, Ghosh S, Dwivedi KK, Khathing DT, Ramachandran TV (1999) Concentration of radon and thoron in some dwellings of the north-eastern region in India. *Indoor Built Environ* 8:322–326
35. Prasad G, Prasad Y, Gusain GS, Ramola RC (2008) Measurement of radon and thoron levels in soil, water and indoor atmosphere of Budhakedar in Garhwal Himalaya, India. *Radiat Meas* 43:S375–S379
36. Misdaq MA, Amrane M, Ouguidi J (2010) Concentrations of  $^{222}\text{Rn}$ ,  $^{220}\text{Rn}$  and their decay products measured in outdoor air in various rural zones (Morocco) by using solid-state nuclear track detectors and resulting radiation dose to the rural populations. *Radiat Prot Dosim* 138(3):223–236
37. Bochicchio F, Ampollini M, Antignani S, Bruni B, Quarto M, Venoso G (2009) Results of the first 5 years of a study on year-to-year variations of radon concentration in Italian dwellings. *Radiat Meas* 44:1064–1068
38. Manousakas M, Fouskas A, Papaefthymiou H, Koukoulidou V, Siavalas G, Kritidis P (2010) Indoor radon measurements in a Greek city located in the vicinity of lignite-fired power plants. *Radiat Meas* 45:1060–1067
39. ICRP (1993) Protection against  $^{222}\text{Rn}$  at home and at work. ICRP Publication 65. *Ann. ICRP* 23(2). Pergamon
40. Chougaonkar MP, Eappen KP, Ramachandran TV, Shetty PG, Mayya YS, Sadasivan S, Venkat Raj V (2004) Profiles of doses to the population living in the high background radiation areas in Kerala, India. *J Environ Radioact* 71:275–297
41. Gusain GS, Prasad G, Prasad Y, Ramola RC (2009) Comparison of indoor radon level with radon exhalation rate from soil in Garhwal Himalaya. *Radiat Meas* 44:1032–1035
42. Bajwa BS, Singh H, Singh J, Singh S, Walia V (2008) A combination study of indoor radon and gamma radiation levels in Tusham ring complex. *Radiat Meas* 43:S475–S478
43. Celik N, Poffijn A, Cevik U, Schepens L (2008) Indoor radon survey in dwellings of the Kars Province, Turkey. *Radiat Prot Dosim* 128(4):432–436